Open access e-Journal **Earth Science India**, Vol. 3 (III), July, 2010, pp. 181-194
http://www.earthscienceindia.info/; eISSN: 0974 – 8350

Chemistry of Tourmalines from the Gangotri Granite, Garhwal Higher Himalaya

T. N. Jowhar
Wadia Institute of Himalayan Geology
33 GMS Road, Dehra Dun 248 001
E-mail: tnjowhar@wihg.res.in; tnjowhar@rediffmail.com

Abstract

The Gangotri granite (23 $\pm$ 0.2 Ma) is one of the largest bodies of the High Himalayan Leucogranite belt (HHL) located in the Garhwal Himalaya. The Gangotri granite is situated structurally above the kyanite and sillimanite gneisses of the Vaikrita Group, which in turn, overlies the north-dipping Main Central Thrust Zone of inverted metamorphic isograds. Compared to other High Himalayan leucogranites, it is particularly enriched in tourmaline. This study focuses especially on mineral chemistry of tourmalines from the Gangotri granite. The Gangotri granite is composed of quartz+ K-feldspar+plagioclase+tourmaline+muscovite $\pm$ biotite $\pm$ garnet $\pm$ beryl, with apatite as the most abundant accessory mineral. K-feldspar is microcline with microperthite. Tourmaline contains inclusions of plagioclase, apatite and monazite. All the analysed tourmalines belong to Alkali Group and are Schorl. Aluminum in T sites varies from 0.000 to 0.202. In Y sites, Al varies from 0.186 to 0.491, Mg from 0.037 to 0.684, Fe^{2+} from 1.639 to 2.218, Mn from 0.000 to 0.041 and Ti from 0.049 to 0.171. In X sites Na varies from 0.619 to 0.777 and (Na + Ca + K) from 0.645 to 0.831. These tourmalines are zoned and from core to rim Mg decreases whereas Fe^{2+}, Ti, Mn and Ca increase. There is a negative correlation between Mg and Fe^{2+}. These results show that there were changes in physical conditions with increased activity of boron during crystallization of the leucogranite magma. Application of two-feldspar geothermometer gives temperatures of subsolidus equilibration at about 441-270^0 C and plagioclase-muscovite gives temperature in the range of 448-339^0 C.

Introduction

The importance of tourmaline for petrologic and metallogenetic studies is well established (*e.g.* Grew and Anovitz, 1996; Henry and Dutrow, 1996; London *et al.,* 1996). Tourmaline is stable over a wide range of pressures and temperatures and has a variable composition and is able to exchange components and volatile species with coexisting minerals and fluids as a result of changes in external conditions. Tourmaline is, therefore useful to monitor the physical and chemical environments in which it was developed (Manning, 1982; London and Manning, 1995; Keller *et al.,* 1999). This study focuses especially on mineral chemistry of tourmalines from the Gangotri granite (Fig.1) and associated pegmatites, which represent one of the Higher Himalayan Leucogranites. The Higher Himalayan Leucogranite Belt (HHL) is a result of the collision-related felsic magmatism with a strong peraluminous character having muscovite $\pm$ biotite and tourmaline. These leucogranites are of great interest as they help us to understand evolution of the continental crust.

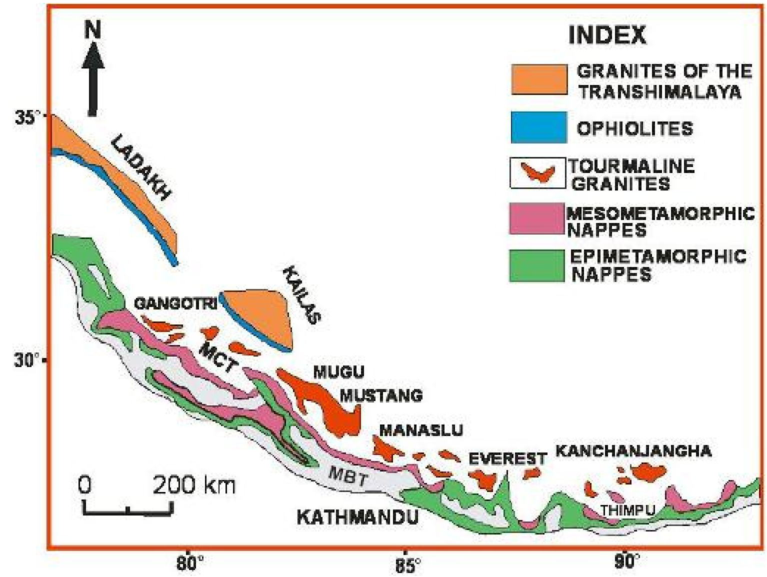

Fig.1: Map showing the distribution of Higher Himalayan Leucogranites (Tourmaline Granites) in the Himalaya.

Geological Setting

The Gangotri granite (Figs. 1 and 2) (23 $\pm$ 0.2 Ma, Searle *et al.,* 1999) is one of the largest bodies of the Higher Himalayan Leucogranite (HHL) belt located in the Garhwal Himalaya (Heim and Gansser, 1939; Gansser, 1964; Le Fort, 1975; Yin, 2006). It is exposed along the upper reaches of the Bhagirathi River around the Gangotri glacier region, including the peaks of Thalay Sagar (6904m), Bhagirathi (6856m), Meru (6672m), Shivling (6543m) and Bhigupanth (6044m). The granite was first described by Heim and Gansser (1939) near the village of Badrinath in the upper Alaknanda valley (Jowhar, 1994; Jowhar and Verma, 1995). Later, Auden (1949) described this granite as composed of tourmaline+muscovite+ biotite + garnet from the upper Bhagirathi valley, and is commonly termed as the Gangotri granite (GG). The Gangotri granite is commonly emplaced as lenses, dykes or as small plutons, which are 1.5-2 km thick and 4-5 km long in contrast to a single Manaslu pluton (Scaillet *et al.,*1990, 1995; Searle *et al.,*1993, 1999).The lenses intrude either the metamorphosed base of the Tethyan Sedimentary Zone, here called the Harsil Formation (Pant, 1986) or in a large body of two-mica porphyritic granite, which has been named as Bhaironghati granite (BG) by Pant (1986). Table-1 gives the lithotectonic setting of the Himalayan metamorphic belt in Garhwal Himalaya. Stern *et al.* (1989) noted that the petrographic and geochemical characteristics of BG are very similar to that of the Cambro-Ordovician felsic magmatism defined by Le Fort *et al.* (1986) in the entire Himalayan belt. The leucogranite is a viscous near-minimum melt, emplaced along foliation parallel laccolith via a dyke network not far from its source region. It was emplaced at mid-crustal depths along the footwall of the Jhala fault, a large-scale low-angle normal fault (part of the STD system), above kyanite and sillimante grade gneisses (Searle *et al.,* 1999).

Open access e-Journal **Earth Science India**, Vol. 3 (III), July, 2010, pp. 181-194
http://www.earthscienceindia.info/; eISSN: 0974 – 8350

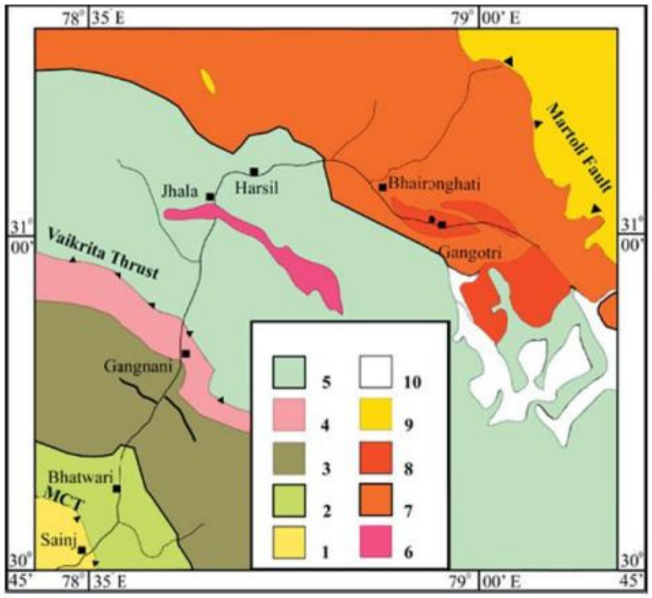

Fig.2: Geological map of the Higher Himalayan Crystalline (HHC) Belt along the Bhagirathi Valley, Garhwal. Legend: 1: Lesser Himalayan (LH) Proterozoic sequence; 2: Higher Himalayan Crystallines (HHC), Bhatwari Group-porphyroclastic granite gneiss, garnetiferous mica schist, amphibolites; 3: mylonitized augen gneiss, mica schist, amphibolite, 4: phyllonite, schist, 5: sillimanite/kyanite/staurolite/garneti-ferous schist/gneiss/migmatite, 6: augen gneiss, 7: Bhaironghati granite, 8: Gangotri leucogranite. 9: Tethyan Sedimentary Zone (Martoli Group). 10: Glaciers, debri etc. Abbreviations: MCT - Main Central Thrust, VT - Vaikrita Thrust, MF - Martoli Fault (from Singh *et. al.,* 2003).

Table-1: Lithotectonic setting of the himalayan metamorphic belt, Garhwal Himalaya.

Tectonic unit	**Lithostratigraphic unit**	**Lithology**
Tethyan Sedimentary Zone	Martoli Formation	Slate-phyllite-quartzite
	---Martoli Fault--	
Himalayan Metamorphic Belt (HMB)	Higher Himalayan Crystalline Belt (HHC)	Gangotri Granite Bhaironghati biotite granite Megacrystic augen gneiss Sill/Ky/grt/bio/mu schist Gneiss, migmatite (Harsil metamorphics) -------- Vaikrita Thrust----- Phyllonite and chlorite schist Mylonitized megacrystic augen gneiss, mica schist amphibolite-metadolerite
	---Main Central Thrust---	
Lesser Himalayan Sedimentary Zone	Garhwal Group	Orthoquartzite-slate-phyllite-dolomite-volcanics

These two distinct granites (GG and BG) are exposed along the road section from Jangla to Gangotri and beyond. The GG is tourmaline-bearing leucogranite whereas BG is biotite granite/gneiss. At the Jangla bridge, biotite granite is deformed to a medium and coarse-grained granite gneiss at the lower structural levels, close to the contact with the Harsil metamorphics. This granite is strongly foliated to granite gneiss along the contact with the metamorphics. Numerous veins of tourmaline-muscovite leucogranite and garnet-beryl-tourmaline pegmatite intruded the biotite granite and the metamorphics. The temple at Gangotri is built on the tourmaline bearing leucogranite (Jain *et al.,* 2002). The GG intrudes both the BG and the Martoli Formation of the Tethyan Sedimentary Zone. The tourmaline bearing leucogranites cut the foliation of the surrounding older biotite granite gneiss and porphyritic granite (Bhaironghati granite) and metasedimentary host rocks. High Himalayan leucogranites in this area yield Th-Pb monazite ages of 22.4 $\pm$ 0.5 Ma (Gangotri), 21.9 $\pm$ 0.5 Ma (Shivling; Harrison et al. 1997), 23.0 $\pm$ 0.2 Ma (Shivling U-Pb age, Searle *et al.,* 1999), whereas 17-22 Ma $^{40}Ar/^{39}Ar$ mica ages were obtained for MCT zone and Higher Himalayan Crystallines (Metcalfe, 1993). Table-2 shows summary of the main tectonic processes and timing constraints for the Garhwal Himalaya and the leucogranite (Prince *et al.,* 1994, Searle *et al.,* 1999).

Sorkhabi *et al.* (1996,1999) documented quantitatively the cooling and denudation history of the Gangotri granites based on fission-track (FT) and $^{40}Ar/^{39}Ar$ ages. Muscovite $^{40}Ar/^{39}Ar$ age of 17.9 $\pm$ 0.1 Ma and a biotite age of 18 $\pm$ 0.1 Ma reflect cooling of the rocks through 300-350 ^{0}C, which is related to an Early Miocene pulse of denudation caused by a basement-cover detachment (the Martoli Normal Fault) above the leucogranites. A total of 15 apatite ages from a vertical profile (2580-4370m) on the Gangotri granites yielded FT ages in the range of 1.5 $\pm$ 0.6 to 2.4 $\pm$ 0.5 Ma, indicating that the rock column with a relief of 1800m cooled through 130 $\pm$ 10 ^{0}C within only one million years during the Late Pliocene. They estimated an average denudation rate of 2 mm/yr for the past 2.4 million years. It is interpreted from these studies that there was one major pulse of tectonic denudation in Early Miocene and another erosional denudation in the Late Pliocene-Quaternary. Searle *et al.* (1999) also reported from the North Ridge of Shivling (from >5000m) K-Ar muscovite ages of 22 $\pm$ 1.0 Ma, fission track ages of zircons are 14.2 $\pm$ 2.1 and 8.8 $\pm$ 1.2 Ma and for apatites are 3.5 $\pm$ 0.79 and 2.61 $\pm$ 0.23 Ma. They also interpret very rapid cooling of the granite at rates of 200-350^0 C/Ma between 23-21 Ma, and tectonic unroofing and erosion removed 24-28 km of overburden during this time. Slow steady state cooling at rates of 20-30^0 C/Ma from 20-1 Ma shows that maximum erosion rates and unroofing of the leucogranite occurred during the early Miocene. This timing coincides with initiation of low-angle, north-dipping normal faulting along the South Tibetan Detachment system.

Table-2: Summary of the timing of tectonic processes in the Garhwal Himalaya (after Searle *et al.,* 1999)

Time	Process
50-37 Ma	Crustal thickening and prograde metamorphism
37 Ma	Peak metamorphism
37-23 Ma	High-temperature sillimanite-grade metamorphism
23 Ma	Crustal anatexis; crystallization of leucogranite
23-21 Ma	Very rapid cooling (~ 175-350 ^{0}C/Ma) of leucogranite; initiation of normal faulting at top of slab along the STD
21-19 Ma	Ductile motion along the MCT shear zone along base of the slab
20-14 Ma	Slow steady cooling at ~ 30^0 C/Ma
14-1 Ma	Very slow cooling at ~ 16-20^0 C/Ma
1-0 Ma	Rapid erosion of upper 2-3 km of the slab by glacial erosion

Petrography

The Gangotri Granite (GG) is fine grained (1-2mm) composed of quartz + K-feldspar + plagioclase + tourmaline + muscovite ± biotite ± garnet ± beryl, with apatite as the most abundant accessory mineral (Fig.3). The GG is subdivided into two main types (i) biotite-granite: It is restricted to the boundary of the plutonic lenses, here biotite is the dominant ferromagnesian phase with subordinate tourmaline, and (ii) tourmaline facies: It is tourmaline-rich and the biotite is absent at a macroscopic scale. Tourmaline occurs as black euhedral-subhedral crystals up to 1cm in size, scattered throughout the granite or concentrated along layers by magmatic banding and can reach up to 5 modal%. It contains abundant inclusions of quartz, plagioclase and apatite. Biotite is restricted to the margins of the leucogranite bodies and reaches up to 2-3%. Biotite is enclosed in plagioclase, K-feldspar, muscovite and quartz. Both micas and tourmaline are in textural equilibrium and there is no evidence for late metasomatic activity in the main leucogranite body.

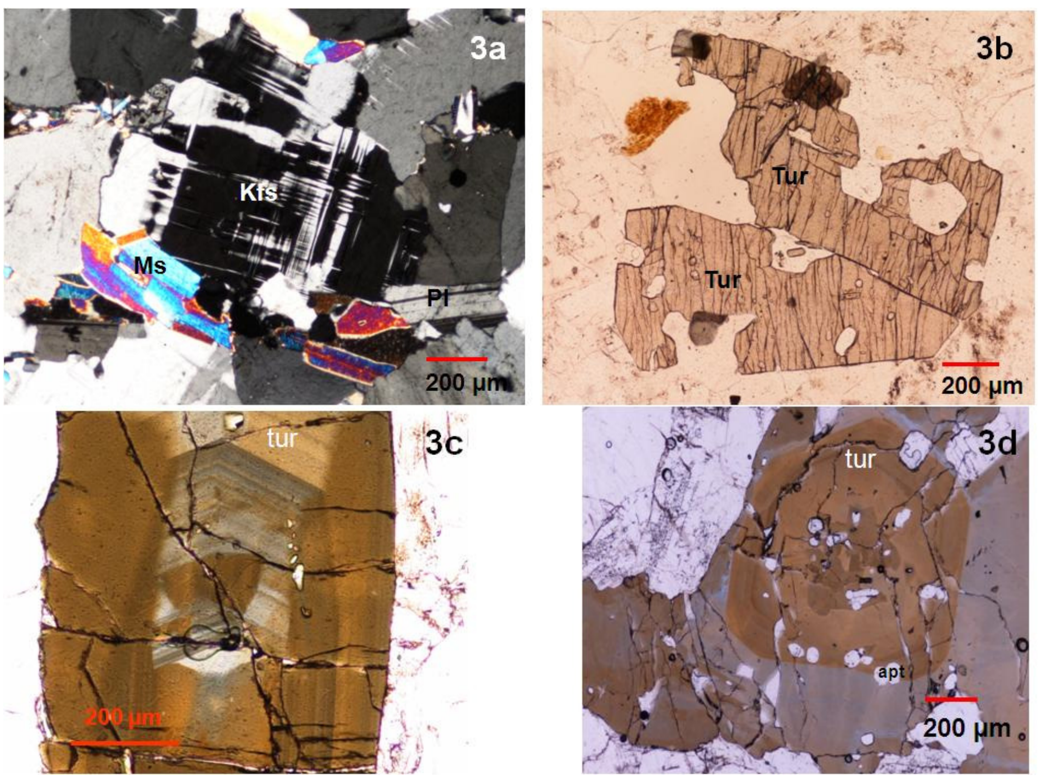

Fig. 3: Photomicrographs of Gangotri granite. (a) Showing quartz (qtz), microcline showing cross-hatched twinning (kfs) and plagioclase (pl) under cross polars (sample no. UG 38); (b) Tourmaline (tur) in plane polarized light (sample no. UG 34); (c) Tourmaline (tur) showing zoning in plane polarized light (sample no. UG33); (d) Tourmaline (tur) showing zoning with inclusions of apatite (apt) (sample no. UG37).

Muscovite is present in both varieties of GG, and its abundance decreases from the biotite to the tourmaline facies (from 13-10%, to 4-5% modal) of GG. Muscovite is mainly enclosed in plagioclase and K-feldspar and is in textural equilibrium with all the other phases. Plagioclase occurs as euhedral-subhedral crystals and contains inclusions of biotite, muscovite, tourmaline and grains of rounded apatite. Optical zonation is extremely rare. K-feldspar is characterized by anhedral habit and contains abundant inclusions of quartz and plagioclase. Exsolution lamellae are very thin. Quartz is homogeneously distributed as interstitial phase. Apatite, zircon and monazite are present in accessory amounts. Apatite is the most abundant accessory mineral and occurs as rounded crystals of 100-200 um in diameter (Fig. 3d). Zircon is present as inclusions in apatite, biotite and muscovite. Monazite occurs as inclusions in apatite and K-feldspar. Opaque minerals are very scarce.

Biotite, muscovite, plagioclase, tourmaline and quartz begin to crystallize early. K-feldspar is xenomorphic in habit and with abundant inclusions and therefore, crystallized late in the sequence. In GG, biotite and plagioclase are magmatic rather than restitic because, the biotite is poor in inclusions when compared to the biotite of paragneisses and the fact that plagioclase show rare optical zonation. Since tourmaline and muscovite define a magmatic layering, this implies they are of magmatic origin.

Mineral Chemistry

The mineral analyses were performed with Cameca SX50 microprobe at Geological Survey of India, Faridabad and Cameca SX100 at Wadia Institute of Himalayan Geology, Dehra Dun. A probe current of 20 nA at an accelerating voltage of 15 KeV and a beam size of 1 microns were used. Standardization was conducted against natural standards using ZAF corrections after Philibert (1963). Representative microprobe analyses of tourmalines, plagioclaes, K-feldspar and muscovites from the Gangotri granite are given in Tables 3, 4, 5 and 6 respectively.

Tourmaline: Representative microprobe analyses of tourmalines from the Gangotri granite are given in Table-3. Cations were calculated on the basis of 24.5 oxygens using a computer program CLASTOUR by Yavuz *et al.* (2002). All the analysed tourmaline belongs to Alkali Group and is Schorl. Aluminum in T sites varies from 0.000 to 0.202. In Y sites, Al varies from 0.186 to 0.491, Mg from 0.037 to 0.684, Fe^{2+} from 1.639 to 2.218, Mn from 0.000 to 0.041 and Ti from 0.049 to 0.171. In X sites Na varies from 0.619 to 0.777 and (Na + Ca + K) from 0.645 to 0.831. These tourmalines are zoned (Figs. 3c and 3d) and from core to rim Mg decreases, Fe^{2+}, Ti, Mn and Ca increases. There is a negative correlation between Mg and Fe^{2+}.

Plagioclases: Plagioclases are rich in albite component, X_{AB} varies from 0.934 to 0.984 and X_{AN} varies from 0.014 to 0.058.

K-feldspar: In K-feldspar (microcline microperthite, Fig. 3a) X_{OR} varies from 0.904 to 0.975 and X_{AB} varies from 0.025 to 0.096. Both plagioclase and K-feldspar from Gangotri granite can be treated as binary solid solutions.

Muscovites: In muscovites Al(IV) varies from 1.561 to 1.793, Al(VI) from 3.503 to 3.658, Fe^{2+} from 0.272 to 0.457, Mg from 0.065 to 0.290 and Na from 0.037 to 0.117.

Geothermometry

The geothermometric calculations were made using two feldspar thermometry in order to estimate the temperature of chemical re-equilibration of feldspars as the feldspars grew and re-equilibrated at different stages of teconothermal history of the Gangotri granite. The methods of Stormer (1975), Whitney and Stormer (1977), Powell and Powell (1977) and Perchuk *et al.* (1991) were followed (Table-7). The plagioclase-alkali feldspar geothermometer formulated by Stormer (1975) does not take into account the effect of calcium in the alkali feldspar. Powell and Powell (1977) calibration takes into account the Ca content of the alkali feldspars. Since there is very little X_{AN} in both plagioclase and K-feldspar from Gangotri granite, they can be treated as binary solid solutions and it is important to note that same temperature estimates are obtained by using Stormer (1975) and Powell and Powell (1977) geothermometric calibrations (Table-7). The temperatures calculated by two-feldspar thermometry gives temperature of subsolidus equilibration and it varies from 441 to 270^0 C. Plagioclase-muscovite geothermometer of Green and Usdansky (1986) was also utilized, and it gives temperature estimates in the range of 448-339^0 C (Table-7).

Conclusions

Mineralogical studies on tourmalines from Gangotri granite reveals that they belong to Alkali Group and are Schorl. These tourmalines are zoned and from core to rim, Mg decreases, Fe^{2+}, Ti, Mn and Ca increases. There is a negative correlation between Mg and Fe^{2+}. These results show that there were changes in physical conditions during crystallization of the leucogranite magma. Further thermodynamic modelling of zoned tourmalines is in progress, which will establish the variation in intensive parameters during crystallization of leucogranite magma. Application of two-feldspar geothermometer gives temperature of subsolidus equilibration of 441-270^0 C and plagioclase-muscovite gives temperature in the range of 448-339^0 C.

Acknowledgements: I wish to express my thanks to Dr. N. C. Pant, Mr. A. Kundu and Ms. Anubhooti Saxena for their help in EPMA analysis and Prof. Santosh Kumar, Kumaon University, Nainital, for valuable suggestions. The facilities and encouragement provided by Dr. A. K. Dubey, Director, Wadia Institute of Himalayan Geology, Dehra Dun, to carry out this research work are thankfully acknowledged.

Appendix: Table- 3 to 7 at the end of the paper.

References

Auden, J. B. (1949) Tehri Garhwal and British Garhwal. Records of the Geological Survey of India , v.76, pp.74-78.

Gansser, A. (1964) Geology of the Himalayas. 289 p., Interscience, New York.

Green, N. L. and Usdansky, S. I. (1986) Towards a practical plagioclase-muscovite thermometer. American Mineralogist, v. 71, pp.1109-117.

Grew, E. S. and Anovitz, L. M. (1996) Boron: mineralogy, petrology and geochemistry. Mineralogical Society of America, Reviews in Mineralogy v.33.

Harrison, T. M., Grove, M. and Lovera, O. M. (1997) New insights into the origin of two contrasting Himalayan granite belts. Geology, v.25, pp.899-902.

Heim, A. and Gansser, A. (1939) The Central Himalayas: Geological observations of the Swiss Expedition of 1936. Mem. Soc. Helv. Sci. Nat., v.73**,** pp.1-245.

Henry, D. J. and Dutrow, B. L. (1996) Metamorphic tourmaline and its petrologic applications. In: *E. S. Grew and L. M. Anovitz (eds.)* Boron: mineralogy, petrology and geochemistry. Mineralogical Society of America, Reviews in Mineralogy, v.33, pp.503-557.

Jain, A. K., Singh, S. and Manickavasagam, R. M. (2002) Himalayan Collision Tectonics. Gondwana Research Group. Memoir No. 7, 114p.

Jowhar, T. N. (1994) Crystal parameters of K-feldspar and geothermometry of the Badrinath Crystalline Complex, Himalaya, India. Neues Jahrbuch fur Mineralogie Abhandlungen, v.166, pp.325-342.

Jowhar, T. N. and Verma, P. K. (1995) Alkali feldspars from the Badrinath Crystalline complex and their bearing on the Himalayan Metamorphism. The Indian Mineralogist, v.29, pp.1-12.

Keller, P., Robles, E. R., Perez, A. P. and Fontan, F. (1999) Chemistry, paragenesis and significance of tourmaline in pegmatites of the Southern Tin belt, Central Namibia. Chemical Geology, v.158**,** pp.203-225.

Le Fort, P. (1975) Himalayas: the collided range, present knowledge of the continental arc. American J. Science, v.275**,** pp.1-44.

Le Fort, P., Debon, F., Pecher, A., Sonet, J. and Vidal, P. (1986) The 500 Ma magmatic event in alpine southern Asia, a thermal episode at Gondwana scale. Sciences de la Terre, v.47**,** pp.191-209.

London, D. and Manning, D. A. C. (1995). Chemical variation and significance of tourmaline from Southwest England. Economic Geology, v.90**,** pp.495-519.

London, D., Morgan VI, G. B., and Wolf, M. B. (1996) Boron in granitic rocks and their contact aureoles. In: *E. S. Grew and L. M. Anovitz (eds.)* Boron: mineralogy, petrology and geochemistry. Mineralogical Society of America Reviews in Mineralogy, v.33**,** pp. 299-330.

Manning, D. A. C. (1982) Chemical and morphological variation in tourmalines from the Hub Kapong batholith of peninsular Thailand. Mineralogical Magazine, v.45**,** pp.139-147.

Metcalfe, R. P. (1993) Pressure, temperature and time constraints on metamorphism across the Main Central Thrust zone and High Himalayan Slab in the Garhwal Himalaya. In: *P.J. Treloar, and M. P. Searle (eds.)* Himalayan Tectonics. Geological Society of London Special Publication, v.74, pp. 485-509.

Pant, R. (1986) Petrochemistry and petrogenesis of the Gangotri granite and associated granitoids, Garhwal Himalaya. Ph.D. Thesis, University of Roorkee, Roorkee, India.

Perchuk, L. L., Podlesskii, K. K. and Aranovich, L. Y. (1991) Thermodynamics of some framework silicates and their equilibria: application to geothermobarometry. In: *L.L. Perchuk (ed.)* Progress in Metamorphic and Magmatic Petrology, A Memorial volume in Honour of D. S. Korzhinskiy. Cambridge University Press, Cambridge, pp.131-164.

Philibert, J. (1963) X-ray optics and X-ray microanalysis. 329p., Academic Press, New York.

Powell, M. and Powell, R. (1977) Plagioclase-alkali feldspar geothermometry revisited. Mineralogical Magazine, v. 41, 253-256.

Prince, C. I., Vance, D. and Harris, N., (1994). Timing of metamorphism in the Garhwal Himalaya. Mineralogical Magazine, L62a, pp.1210-1211.

Scaillet, B., France-Lanord, C. and Le Fort, P., (1990). Badrinath-Gangotri plutons (Garhwal, India): petrological and geochemical evidence for fractionation processes in a high Himalayan leucogranite. Journal of Volcanology and Geothermal Research, v.44, pp.163-188.

Scaillet, B., Pecher, A., Rochette, P. and Champenois, M. (1995) The Gangotri granite (GarhwaHimalaya): laccolithic emplacement in an extending collisional belt. J. Geophysical Research, v.100, pp.585-607.

Searle, M. P., Metcalfe, R. P., Rex, A. J. and Norry, M. J. (1993) Field relations, petrogenesis and emplacement of the Bhagirathi leucogranite, Garhwal Himalaya. In: *P. J. Treloar and M. P. Searle (eds.)* Himalayan Tectonics. Geological Society of London Special Publication, v.74, pp. 429-444.

Searle, M. P., Noble, S. R., Hurford, A. J. and Rex, D. C. (1999) Age of crustal melting, emplacement and exhumation history of the Shivling leucogranite, Garhwal Himalaya. Geological Magazine, v.136, pp.513-525.

Singh, S., Mukherjee, P. K., Jain, A. K., Khanna, P. P., Saini, N. K. and Kumar, Rajeev (2003)Source characterization and possible emplacement mechanism of collision-related Gangotri leucogranite along Bhagirathi valley, NW-Himalaya. In: *S. Singh (ed.)* Granitoids of the Himalayan Collision belt. J. Virtual Explorer, v.11, pp. 60-73.

Sorkhabi, R. B., Stump, E., Foland, K. A. and Jain, A. K. (1996) Fission-track and $^{40}Ar/^{39}Ar$ evidence for episodic denudation of the Gangotri granites in the Garhwal Higher Himalaya, India. Tectonophysics, v.260, pp.187-199.

Sorkhabi, R. B., Stump, E., Foland,K.A. and Jain, A. K. (1999) Tectonic and cooling history of the Garhwal Higher Himalaya (Bhagirathi Valley): constraints from thermochronological data. In: *A. K. Jain and R. M. Manickavasagam (eds.)* Geodynamics of the NW Himalaya. Gondwana Research Group Memoir, v.6, pp. 217-235.

Stern, C. R., Kligfield, R., Schelling, D., Virdi, N. S., Futa, K., Peterman, Z. E. and Amini, H. (1989) The Bhagirathi leucogranite of the High Himalaya (Garhwal, India): age, petrogenesis and tectonic implications. Geological Society of America, Special Publications, v.232, pp.33-45.

Stormer, J. C., Jr. (1975) A practical two-feldspar geothermometer. American Mineralogist, v. 60, pp. 667-674.

Whitney, J. A. and Stormer, J. C., Jr. (1977) The distribution of $NaAlSi_3O_8$ between coexisting microcline and plagioclase and its effect on geothermometric calculations. American Mineralogist, v. 62, pp.687-691.

Yavuz, F., Gultekin, A. H. and Karakaya, M. C. (2002) CLASTOUR: a computer program for classification of the minerals of the tourmaline group. Computers and Geosciences, v.28, pp.1017-1036.

Yin, A. (2006) Cenozoic tectonic evolution of the Himalayan orogen as constrained by along-strike variation of structural geometry, exhumation history, and foreland sedimentation. Earth Science Reviews, v.76, pp.1-131.

Table 3. Representative microprobe analyses of tourmalines from Gangotri granite

	UG33/1	UG33/1	UG33/2	UG33/2	UG33/3	UG33/3	UG37/1	UG37/1
	CORE	RIM	CORE	RIM	CORE	RIM	CORE	RIM
SiO2	35.16	34.83	35.14	34.90	35.26	34.46	34.99	34.43
TiO2	0.39	0.69	0.69	0.58	0.52	0.76	0.65	1.34
Al2O3	32.91	32.33	32.24	31.72	32.97	32.68	32.44	31.56
Cr2O3	0.03	0.00	0.08	0.00	0.00	0.07	0.01	0.00
FeO	14.97	14.46	14.26	15.61	14.07	14.98	13.41	14.57
MnO	0.17	0.05	0.08	0.17	0.15	0.18	0.12	0.19
MgO	1.22	1.72	1.52	1.29	1.61	1.38	2.14	1.68
CaO	0.11	0.27	0.20	0.25	0.15	0.19	0.20	0.27
Na2O	1.93	1.96	2.13	2.10	2.00	2.02	2.17	2.21
K2O	0.06	0.05	0.06	0.03	0.09	0.06	0.06	0.09
Total	86.94	86.37	86.39	86.63	86.81	86.77	86.20	86.34
	CATIONS	PER 24.5	OXYGENS					
Si	5.915	5.895	5.938	5.930	5.916	5.829	5.905	5.858
Al (T)	0.085	0.105	0.062	0.070	0.084	0.171	0.095	0.142
SUM T	6.000	6.000	6.000	6.000	6.000	6.000	6.000	6.000
Al (Z)	6.000	6.000	6.000	6.000	6.000	6.000	6.000	6.000
Mg	0.306	0.434	0.383	0.327	0.403	0.348	0.539	0.426
Fe2+	2.106	2.046	2.015	2.218	1.974	2.119	1.894	2.073
Mn	0.024	0.007	0.011	0.024	0.021	0.026	0.018	0.027
Al (Y)	0.440	0.343	0.359	0.282	0.434	0.343	0.356	0.186
Ti	0.049	0.088	0.088	0.074	0.066	0.097	0.082	0.171
Cr3+	0.004	0.000	0.011	0.000	0.000	0.009	0.002	0.000
SUM Y	2.930	2.918	2.867	2.925	2.898	2.941	2.890	2.883
Ca	0.020	0.049	0.036	0.046	0.027	0.034	0.036	0.049
Na	0.629	0.643	0.698	0.692	0.651	0.662	0.709	0.729
K	0.013	0.011	0.013	0.007	0.019	0.013	0.012	0.020
SUM X	0.662	0.703	0.747	0.744	0.697	0.710	0.757	0.798
CATIONS	15.592	15.621	15.614	15.669	15.595	15.651	15.647	15.681

	UG37/2	UG37/2	UG38/1	UG38/1	UG38/2	UG38/2	UG41/1	UG41/1
	CORE	RIM	CORE	RIM	CORE	RIM	CORE	RIM
SiO2	35.07	34.58	34.99	34.32	36.58	35.76	35.71	34.14
TiO2	0.68	0.81	0.79	0.82	0.75	0.81	0.65	0.93
Al2O3	32.85	32.40	31.76	31.42	31.74	31.52	32.37	31.36
Cr2O3	0.00	0.01	0.00	0.00	0.00	0.00	0.00	0.07
FeO	13.45	13.56	12.46	14.04	13.13	13.92	12.26	14.12
MnO	0.09	0.01	0.09	0.20	0.17	0.18	0.06	0.20
MgO	2.29	2.08	2.52	1.60	2.08	1.44	2.74	0.14
CaO	0.21	0.20	0.19	0.23	0.22	0.20	0.19	0.33
Na2O	2.07	2.06	2.20	2.17	2.15	2.09	2.13	1.99
K2O	0.05	0.04	0.06	0.07	0.06	0.06	0.06	0.07
Total	86.75	85.74	85.03	84.85	86.86	85.95	86.17	83.35
	CATIONS	PER 24.5	OXYGENS					
Si	5.876	5.869	5.957	5.919	6.000	6.000	5.980	5.987
Al (T)	0.124	0.131	0.044	0.081	0.000	0.000	0.020	0.013
SUM T	6.000	6.000	6.000	6.000	6.000	6.000	6.000	6.000
Al (Z)	6.000	6.000	6.000	6.000	6.000	6.000	6.000	6.000
Mg	0.572	0.526	0.640	0.410	0.516	0.363	0.684	0.037
Fe2+	1.884	1.924	1.773	2.025	1.831	1.972	1.717	2.070
Mn	0.013	0.001	0.013	0.029	0.024	0.026	0.009	0.030
Al (Y)	0.362	0.350	0.328	0.303	0.236	0.292	0.368	0.468
Ti	0.086	0.103	0.101	0.106	0.094	0.103	0.082	0.123
Cr3+	0.000	0.001	0.000	0.000	0.000	0.000	0.000	0.010
SUM Y	2.916	2.907	2.855	2.872	2.700	2.754	2.858	2.737
Ca	0.038	0.036	0.034	0.043	0.039	0.036	0.034	0.062
Na	0.672	0.678	0.726	0.726	0.695	0.687	0.691	0.677
K	0.011	0.009	0.012	0.016	0.012	0.012	0.013	0.016
SUM X	0.721	0.723	0.772	0.784	0.746	0.734	0.738	0.754
CATIONS	15.637	15.630	15.627	15.656	15.446	15.488	15.596	15.491

	UG41/2	UG41/2	UG42/2	UG42/2	UG42/1
	CORE	RIM	CORE	RIM	RIM
SiO2	35.21	34.39	34.55	34.04	34.48
TiO2	0.90	1.14	0.54	0.72	0.86
Al2O3	32.01	32.08	32.67	31.91	31.77
Cr2O3	0.03	0.00	0.01	0.05	0.08
FeO	13.19	14.34	13.51	14.82	14.80
MnO	0.13	0.13	0.18	0.22	0.16
MgO	2.32	1.29	1.80	1.30	1.38
CaO	0.19	0.38	0.19	0.35	0.37
Na2O	2.22	2.07	2.04	2.21	2.02
K2O	0.03	0.10	0.04	0.11	0.06
Total	86.23	85.92	85.53	85.73	85.98
	CATIONS	PER 24.5	OXYGENS		
Si	5.934	5.863	5.878	5.843	5.888
Al (T)	0.066	0.137	0.122	0.157	0.112
SUM T	6.000	6.000	6.000	6.000	6.000
Al (Z)	6.000	6.000	6.000	6.000	6.000
Mg	0.583	0.328	0.456	0.333	0.351
Fe2+	1.859	2.044	1.922	2.127	2.113
Mn	0.019	0.019	0.026	0.032	0.023
Al (Y)	0.292	0.309	0.428	0.298	0.282
Ti	0.114	0.146	0.069	0.093	0.110
Cr3+	0.004	0.000	0.001	0.007	0.011
SUM Y	2.870	2.846	2.902	2.889	2.891
Ca	0.034	0.069	0.035	0.064	0.068
Na	0.725	0.684	0.673	0.735	0.669
K	0.006	0.022	0.009	0.024	0.013
SUM X	0.766	0.775	0.716	0.824	0.750
CATIONS	15.636	15.621	15.618	15.713	15.641

Open access e-Journal **Earth Science India**, Vol. 3 (III), July, 2010, pp. 181-194
http://www.earthscienceindia.info/; eISSN: 0974 – 8350

Table 4. Representative microprobe analyses of plagioclase from Gangotri granite

	UG33/1 CORE	UG33/1 RIM	UG33/2 CORE	UG33/2 RIM	UG37/1 CORE	UG37/1 RIM	UG37/2
SiO2	68.11	68.04	67.12	68.98	69.27	68.38	68.82
TiO2	0.00	0.04	0.04	0.00	0.00	0.00	0.00
Al2O3	19.62	19.98	20.06	19.95	20.37	20.30	20.28
Cr2O3	0.02	0.07	0.06	0.03	0.00	0.01	0.07
FeO	0.03	0.00	0.07	0.02	0.00	0.01	0.00
MnO	0.00	0.00	0.04	0.05	0.04	0.03	0.07
MgO	0.00	0.01	0.00	0.01	0.00	0.01	0.03
CaO	0.52	0.86	1.00	0.47	0.64	0.73	0.65
Na2O	11.38	11.19	8.88	11.39	9.88	11.06	10.60
K2O	0.12	0.14	0.10	0.07	0.14	0.18	0.08
Total	99.82	100.31	97.36	100.97	100.34	100.70	100.60
	Cations	per 8	Oxygens				
Si	2.984	2.968	2.989	2.984	2.997	2.968	2.981
Al	1.013	1.027	1.053	1.017	1.039	1.038	1.035
Na	0.966	0.946	0.767	0.955	0.829	0.931	0.890
Ca	0.024	0.040	0.048	0.022	0.030	0.034	0.030
K	0.007	0.008	0.006	0.004	0.008	0.010	0.004
Ti	0.000	0.001	0.001	0.000	0.000	0.000	0.000
Fe2+	0.001	0.000	0.003	0.001	0.000	0.000	0.000
Mg	0.000	0.001	0.000	0.001	0.000	0.001	0.002
Mn	0.000	0.000	0.002	0.002	0.001	0.001	0.003
Cr3+	0.001	0.002	0.002	0.001	0.000	0.000	0.002
Total	4.996	4.993	4.871	4.987	4.904	4.983	4.947
XAB	0.969	0.952	0.934	0.973	0.956	0.955	0.963
XAN	0.024	0.040	0.058	0.022	0.035	0.035	0.032
XOR	0.007	0.008	0.007	0.004	0.009	0.010	0.004

	UG38/1 CORE	UG38/1 RIM	UG38/1A CORE	UG38/1A RIM	UG38/2 CORE	UG38/2 RIM	UG38/3 CORE	UG38/3 RIM
SiO2	68.12	67.62	67.09	68.89	69.34	66.89	67.65	68.14
TiO2	0.02	0.02	0.00	0.02	0.02	0.01	0.01	0.05
Al2O3	19.78	20.08	20.33	19.84	19.93	20.40	20.02	20.02
Cr2O3	0.00	0.00	0.00	0.00	0.00	0.00	0.00	0.00
FeO	0.03	0.08	0.09	0.02	0.05	0.09	0.03	0.07
MnO	0.02	0.03	0.05	0.03	0.01	0.01	0.04	0.00
MgO	0.00	0.01	0.00	0.01	0.00	0.00	0.01	0.01
CaO	0.44	0.50	0.82	0.46	0.44	1.09	0.54	0.53
Na2O	11.30	11.39	11.20	11.31	11.52	11.04	11.50	11.32
K2O	0.10	0.14	0.12	0.09	0.06	0.13	0.13	0.14
Total	99.78	99.85	99.70	100.67	101.37	99.66	99.90	100.28
	Cations	per 8	Oxygens					
Si	2.982	2.964	2.948	2.988	2.988	2.942	2.965	2.972
Al	1.020	1.038	1.053	1.014	1.012	1.057	1.034	1.029
Na	0.959	0.968	0.954	0.951	0.962	0.941	0.977	0.957
Ca	0.021	0.024	0.039	0.021	0.020	0.051	0.025	0.025
K	0.006	0.008	0.007	0.005	0.003	0.007	0.007	0.008
Ti	0.001	0.001	0.000	0.001	0.001	0.000	0.000	0.002
Fe2+	0.001	0.003	0.003	0.001	0.002	0.003	0.001	0.003
Mg	0.000	0.001	0.000	0.001	0.000	0.000	0.001	0.001
Mn	0.001	0.001	0.002	0.001	0.000	0.000	0.002	0.000
Cr3+	0.000	0.000	0.000	0.000	0.000	0.000	0.000	0.000
Total	4.989	5.005	5.006	4.983	4.988	5.001	5.010	4.997
XAB	0.973	0.968	0.954	0.973	0.977	0.942	0.968	0.967
XAN	0.021	0.024	0.039	0.021	0.020	0.051	0.025	0.025
XOR	0.006	0.008	0.007	0.005	0.003	0.007	0.007	0.008

	UG41/1 CORE	UG41/1 RIM	UG41/2 CORE	UG41/2 RIM	UG42/2	UG42/2	UG42/2
SiO2	67.59	68.55	67.55	67.84	66.93	66.72	67.21
TiO2	0.00	0.03	0.00	0.03	0.00	0.04	0.00
Al2O3	19.58	19.82	19.94	19.44	19.72	20.08	19.66
Cr2O3	0.00	0.00	0.00	0.00	0.00	0.05	0.00
FeO	0.01	0.19	0.00	0.00	0.14	0.00	0.00
MnO	0.06	0.05	0.00	0.00	0.04	0.09	0.01
MgO	0.00	0.02	0.00	0.01	0.01	0.00	0.00
CaO	0.47	0.31	0.63	0.36	0.61	1.01	0.77
Na2O	11.17	11.43	11.07	11.51	11.09	10.92	11.26
K2O	0.08	0.04	0.13	0.11	0.06	0.10	0.10
Total	99.06	100.54	99.54	99.32	98.63	99.08	99.03
	Cations	per 8	Oxygens				
Si	2.984	2.983	2.972	2.987	2.969	2.951	2.971
Al	1.019	1.016	1.034	1.009	1.031	1.047	1.024
Na	0.956	0.964	0.944	0.982	0.954	0.936	0.965
Ca	0.022	0.014	0.030	0.017	0.029	0.048	0.036
K	0.005	0.002	0.007	0.006	0.003	0.006	0.006
Ti	0.000	0.001	0.000	0.001	0.000	0.001	0.000
Fe2+	0.000	0.007	0.000	0.000	0.005	0.000	0.000
Mg	0.000	0.001	0.000	0.001	0.001	0.000	0.000
Mn	0.002	0.002	0.000	0.000	0.002	0.003	0.000
Cr3+	0.000	0.000	0.000	0.000	0.000	0.002	0.000
Total	4.988	4.990	4.987	5.003	4.994	4.994	5.002
XAB	0.973	0.984	0.962	0.977	0.968	0.945	0.958
XAN	0.022	0.014	0.031	0.017	0.029	0.048	0.036
XOR	0.005	0.002	0.007	0.006	0.003	0.006	0.006

Open access e-Journal **Earth Science India**, Vol. 3 (III), July, 2010, pp. 181-194
http://www.earthscienceindia.info/; eISSN: 0974 – 8350

Table 5. Representative microprobe analyses of K-feldspar from Gangotri granite

	UG33/1	UG33/2	UG33/3	UG37/1 CORE	UG37/1 RIM	UG37/1	UG37/2
SiO2	64.68	65.33	65.25	66.12	64.87	65.19	65.73
TiO2	0.00	0.00	0.03	0.02	0.07	0.00	0.00
Al2O3	18.60	18.69	18.56	18.82	18.21	18.91	18.86
Cr2O3	0.02	0.00	0.10	0.00	0.05	0.00	0.00
FeO	0.04	0.00	0.05	0.01	0.00	0.01	0.02
MnO	0.04	0.01	0.05	0.03	0.00	0.02	0.06
MgO	0.01	0.00	0.00	0.00	0.01	0.01	0.00
CaO	0.00	0.00	0.00	0.00	0.00	0.00	0.00
Na2O	0.51	0.71	0.63	0.78	0.56	0.27	0.36
K2O	15.74	15.64	15.40	15.37	15.84	15.84	15.44
Total	99.65	100.38	100.08	101.14	99.59	100.24	100.47
	Cations	per 8	Oxygens				
Si	2.993	2.997	3.000	3.003	3.004	2.994	3.004
Al	1.014	1.011	1.006	1.007	0.994	1.023	1.016
Na	0.046	0.063	0.056	0.069	0.050	0.024	0.032
Ca	0.000	0.000	0.000	0.000	0.000	0.000	0.000
K	0.929	0.915	0.903	0.891	0.936	0.928	0.900
Ti	0.000	0.000	0.001	0.001	0.002	0.000	0.000
Fe2+	0.002	0.000	0.002	0.000	0.000	0.000	0.001
Mg	0.001	0.000	0.000	0.000	0.001	0.001	0.000
Mn	0.002	0.000	0.002	0.001	0.000	0.001	0.002
Cr3+	0.001	0.000	0.004	0.000	0.002	0.000	0.000
Total	4.988	4.986	4.974	4.972	4.989	4.971	4.955
XOR	0.953	0.936	0.942	0.928	0.949	0.975	0.966
XAB	0.047	0.064	0.058	0.072	0.051	0.025	0.034
XAN	0.000	0.000	0.000	0.000	0.000	0.000	0.000

	UG38/1 CORE	UG38/1 RIM	UG38/2 CORE	UG38/2 RIM	UG38/3 CORE	UG38/3 RIM	UG41/1 CORE	UG41/1 RIM
SiO2	65.83	65.35	65.11	66.13	64.83	66.59	65.08	63.88
TiO2	0.01	0.02	0.00	0.00	0.01	0.00	0.00	0.00
Al2O3	18.30	18.18	18.69	18.38	18.45	18.53	18.24	18.19
Cr2O3	0.00	0.00	0.00	0.00	0.00	0.00	0.04	0.00
FeO	0.06	0.09	0.06	0.10	0.03	0.01	0.06	0.04
MnO	0.02	0.00	0.03	0.02	0.01	0.00	0.00	0.00
MgO	0.00	0.00	0.00	0.01	0.00	0.01	0.02	0.00
CaO	0.00	0.02	0.01	0.00	0.00	0.00	0.00	0.00
Na2O	0.51	0.45	0.88	0.52	0.53	0.67	0.47	0.43
K2O	15.78	16.04	15.10	15.74	15.78	15.30	16.55	16.42
Total	100.50	100.13	99.86	100.88	99.63	100.11	100.52	99.10
	Cations	per 8	Oxygens					
Si	3.016	3.012	2.997	3.016	3.000	3.021	3.000	2.991
Al	0.988	0.988	1.014	0.988	1.006	0.991	0.991	1.004
Na	0.045	0.040	0.078	0.046	0.048	0.059	0.042	0.039
Ca	0.000	0.001	0.000	0.000	0.000	0.000	0.000	0.000
K	0.922	0.943	0.887	0.916	0.932	0.885	0.973	0.981
Ti	0.001	0.001	0.000	0.000	0.000	0.000	0.000	0.000
Fe2+	0.002	0.004	0.003	0.004	0.001	0.001	0.002	0.002
Mg	0.000	0.000	0.000	0.001	0.000	0.001	0.001	0.000
Mn	0.001	0.000	0.001	0.001	0.000	0.000	0.000	0.000
Cr3+	0.000	0.000	0.000	0.000	0.000	0.000	0.001	0.000
Total	4.974	4.986	4.978	4.971	4.986	4.956	5.010	5.017
XOR	0.953	0.958	0.919	0.952	0.951	0.938	0.959	0.962
XAB	0.047	0.041	0.081	0.048	0.049	0.063	0.041	0.038
XAN	0.000	0.001	0.000	0.000	0.000	0.000	0.000	0.000

	UG41/2 CORE	UG41/2 RIM	UG42/1 CORE	UG42/1 RIM	UG42/2	UG42/2	UG42/2	UG42/3	UG42/3	UG42/3
SiO2	63.66	63.55	64.87	64.69	64.21	63.96	61.78	62.54	63.59	64.05
TiO2	0.00	0.00	0.00	0.00	0.00	0.00	0.00	0.00	0.00	0.01
Al2O3	17.89	18.12	18.05	18.21	18.02	18.27	17.28	17.82	18.07	18.48
Cr2O3	0.00	0.09	0.05	0.01	0.00	0.01	3.67	0.08	0.00	0.00
FeO	0.00	0.00	0.01	0.16	0.02	0.06	0.05	0.00	0.01	0.00
MnO	0.04	0.00	0.00	0.00	0.04	0.00	0.00	0.00	0.00	0.00
MgO	0.00	0.00	0.02	0.00	0.01	0.01	0.06	0.01	0.00	0.01
CaO	0.00	0.00	0.00	0.00	0.00	0.03	0.00	0.01	0.00	0.00
Na2O	0.78	0.38	0.70	0.36	0.45	0.41	0.38	0.55	0.55	0.79
K2O	15.96	16.58	16.32	16.46	16.21	16.07	16.12	15.54	16.56	16.07
Total	98.38	98.75	100.08	99.90	98.97	98.85	99.50	96.57	99.08	99.42
	Cations	per 8	Oxygens						Cations	per 8 Oxygens
Si	2.997	2.987	3.003	2.999	3.002	2.993	2.920	2.993	2.988	2.982
Al	0.993	1.004	0.985	0.995	0.993	1.008	0.963	1.005	1.001	1.014
Na	0.071	0.035	0.063	0.032	0.041	0.037	0.035	0.051	0.050	0.071
Ca	0.000	0.000	0.000	0.000	0.000	0.002	0.000	0.001	0.000	0.000
K	0.959	0.994	0.964	0.973	0.967	0.959	0.972	0.949	0.993	0.954
Ti	0.000	0.000	0.000	0.000	0.000	0.000	0.000	0.000	0.000	0.000
Fe2+	0.000	0.000	0.000	0.006	0.001	0.002	0.002	0.000	0.000	0.000
Mg	0.000	0.000	0.001	0.000	0.001	0.001	0.004	0.001	0.000	0.001
Mn	0.002	0.000	0.000	0.000	0.002	0.000	0.000	0.000	0.000	0.000
Cr3+	0.000	0.003	0.002	0.000	0.000	0.000	0.137	0.003	0.000	0.000
Total	5.022	5.023	5.018	5.005	5.007	5.002	5.033	5.003	5.032	5.022
XOR	0.931	0.966	0.939	0.968	0.959	0.961	0.965	0.948	0.952	0.931
XAB	0.069	0.034	0.061	0.032	0.041	0.037	0.035	0.051	0.048	0.069
XAN	0.000	0.000	0.000	0.000	0.000	0.002	0.000	0.001	0.000	0.000

Table 6. Representative microprobe analyses of muscovites from Gangotri granite

	UG33/2 CORE	UG33/2 RIM	UG37/1	UG37/2	UG38/3 CORE	UG38/3 RIM	UG41/2 CORE	UG41/2 RIM
SiO2	47.61	46.67	47.66	48.76	48.27	47.69	45.42	46.17
TiO2	0.23	0.31	0.71	0.17	0.49	0.43	0.53	0.41
Al2O3	34.58	33.96	34.89	34.90	32.95	32.60	33.59	32.56
Cr2O3	0.00	0.01	0.04	0.04	0.00	0.00	0.01	0.00
FeO	3.32	3.45	2.48	2.77	3.51	3.72	3.07	3.80
MnO	0.17	0.07	0.15	0.15	0.17	0.18	0.09	0.15
MgO	0.41	0.38	0.59	1.51	0.34	0.38	0.37	0.53
CaO	0.00	0.02	0.00	0.02	0.00	0.03	0.00	0.04
Na2O	0.34	0.33	0.36	0.26	0.24	0.35	0.31	0.14
K2O	9.72	9.45	9.97	9.55	10.93	10.58	10.12	9.82
Total	96.38	94.65	96.85	98.13	96.89	95.94	93.62	93.64
	Cations	per 22	Oxygens					
Al(Total)	5.377	5.378	5.388	5.305	5.137	5.136	5.410	5.242
Si	6.281	6.271	6.245	6.289	6.386	6.375	6.207	6.307
Al(IV)	1.719	1.729	1.755	1.711	1.614	1.625	1.793	1.693
Total	8.000	8.000	8.000	8.000	8.000	8.000	8.000	8.000
Al(VI)	3.658	3.649	3.633	3.594	3.523	3.511	3.617	3.549
Ti	0.023	0.031	0.070	0.016	0.049	0.043	0.054	0.042
Fe(2+)	0.366	0.388	0.272	0.299	0.389	0.416	0.351	0.434
Mn	0.019	0.008	0.017	0.016	0.019	0.020	0.010	0.017
Mg	0.081	0.076	0.115	0.290	0.067	0.075	0.075	0.108
Cr	0.000	0.001	0.004	0.004	0.000	0.000	0.001	0.000
Total	4.147	4.153	4.111	4.219	4.046	4.064	4.108	4.150
Ca	0.000	0.003	0.000	0.003	0.000	0.004	0.000	0.006
Na	0.087	0.086	0.091	0.065	0.062	0.090	0.082	0.037
K	1.636	1.620	1.666	1.571	1.845	1.804	1.764	1.711
Total	1.723	1.709	1.757	1.639	1.906	1.897	1.846	1.754
Sum Cations	13.870	13.862	13.868	13.858	13.952	13.961	13.954	13.904

	UG42/2	UG42/2	UG42/3	UG42/3	UG42/3
SiO2	45.24	45.22	45.92	45.87	45.39
TiO2	0.40	0.32	0.44	0.33	0.37
Al2O3	33.17	33.13	32.41	31.37	33.27
Cr2O3	0.00	0.00	0.00	0.03	0.00
FeO	3.30	3.59	3.73	3.94	3.23
MnO	0.18	0.07	0.08	0.18	0.13
MgO	0.41	0.41	0.53	0.53	0.40
CaO	0.00	0.00	0.02	0.00	0.00
Na2O	0.33	0.44	0.26	0.28	0.43
K2O	10.43	10.36	9.96	9.73	10.11
Total	93.46	93.60	93.36	92.30	93.46
	Cations	per 22	Oxygens		
Al(Total)	5.368	5.362	5.239	5.134	5.377
Si	6.212	6.210	6.298	6.369	6.225
Al(IV)	1.788	1.790	1.702	1.631	1.775
Total	8.000	8.000	8.000	8.000	8.000
Al(VI)	3.580	3.572	3.537	3.503	3.602
Ti	0.041	0.033	0.045	0.034	0.038
Fe(2+)	0.379	0.412	0.428	0.457	0.370
Mn	0.021	0.008	0.009	0.021	0.015
Mg	0.084	0.084	0.108	0.110	0.082
Cr	0.000	0.000	0.000	0.003	0.000
Total	4.105	4.109	4.127	4.128	4.107
Ca	0.000	0.000	0.003	0.000	0.000
Na	0.088	0.117	0.069	0.075	0.114
K	1.827	1.815	1.743	1.723	1.769
Total	1.915	1.932	1.815	1.798	1.883
Sum Cations	14.020	14.041	13.942	13.926	13.990

Table 7. Temperature estimates from Gangotri granite

	UG33/1	UG33/1	UG33/2	UG33/2	UG37/1	UG37/1
Two Feldspar	CORE	RIM	CORE	RIM	CORE	RIM
1. Whitney & Stormer 1977	398	397	432	427	441	404
2. Stormer 1975	350	349	385	379	394	356
Average of 1 and 2	374	373	408	403	418	380
3. Powell & Powell 1977	350	349	385	380	394	356
4. Perchuk et al. 1991	311	310	352	344	362	318
Plagioclase-Muscovite						
Green & Usdansky 1986			425	366	438	448

	UG37/2	UG41/1	UG41/1	UG41/2	UG41/2	UG42/2
Two Feldspar		CORE	RIM	CORE	RIM	
1. Whitney & Stormer 1977	366	382	373	436	363	375
2. Stormer 1975	316	333	324	388	314	326
Average of 1 and 2	341	357	349	412	339	351
3. Powell & Powell 1977	317	334	325	389	315	326
4. Perchuk et al. 1991	273	292	281	355	270	284
Plagioclase-Muscovite						
Green & Usdansky 1986				404	339	391

T in degree Celsius